Singularity and nonlinearity in the Kapitza resistance between gold and superfluid ^{4}He near T_λ

Robert V. Duncan* and Guenter Ahlers
Department of Physics and Center for Nonlinear Science, University of California, Santa Barbara, California 93106
(Received 22 January 1990; revised manuscript received 5 July 1990)

We report experimental results for the Kapitza resistance R_K between gold and superfluid ^{4}He, which were obtained by using very-high-resolution thermometry. The data imply that R_K is singular at the superfluid transition temperature T_λ. Comparison with theory suggests that the singularity results from a hydrodynamic effect proposed by Landau, and that it is associated with the vanishing of the superfluid and normal-fluid currents at the boundaries. Recently a quantitative prediction of the singular part of this Kapitza resistance has been made based on dynamic renormalization-group theory. This theory requires no adjustable parameters and it agrees well with our data. The measurements of R_K are independent of the heat flux Q only for reduced temperatures $t = 1 - T/T_\lambda$ greater than a characteristic value t_c. We find that t_c is approximately proportional to Q, and that for $t < t_c$ the maximum value of $(\partial R_K/\partial Q)_t$ is approximately proportional to $1/t$. The Q-dependent contribution R_{KQ} to R_K can be represented by a function of the single variable Q/t. For large Q/t, this function saturates at a value near 0.35 cm^2 K/W. We know of no theory that predicts the dependence of R_K on Q.

I. INTRODUCTION

Heat transport in superfluid ^{4}He occurs by counterflow of the normal-fluid and superfluid currents, and at sufficiently small heat currents does not induce any temperature gradient in the bulk liquid.[1] Therefore the temperature difference across a conductivity cell will result only from effects associated with the solid-liquid boundaries and the finite conductivity of the solid endplates of the cell. The thermal resistance R_K associated with the boundaries is the Kapitza resistance,[2] and is generally attributed to a discontinuity of the temperature at the solid-liquid interface. Pollack,[3] Pfotenhauer and Donnelly,[4] Swartz and Pohl,[5] and Swartz[6] have reviewed both experimental and theoretical work on the Kapitza resistance.

Although an anomaly in R_K near the superfluid transition temperature T_λ was mentioned in passing[7] as early as 1953, the systematic study of this boundary effect has been undertaken only recently.[8–17] It has become clear that two apparently separate physical phenomena contribute to the anomaly in R_K. Our measurements show that the zero-heat-current limit R_{K0} of R_K increases by roughly 10% as the reduced temperature $t \equiv 1 - T/T_\lambda$ is decreased from 10^{-3} to 10^{-5}, indicating that R_{K0} is singular at T_λ.[8,11,18] The singularity in R_{K0} is believed to result from a two-fluid hydrodynamic mechanism proposed by Landau.[19] Well within the bulk superfluid, heat is transported by counterflow of the normal-fluid and superfluid components, and hence no thermal gradient exists across the bulk superfluid. At a boundary, say the colder boundary for instance, the incoming normal fluid must be converted to superfluid to preserve counterflow. For reduced temperatures t greater than 10^{-2} this conversion occurs very near the boundary and virtually instantaneously and hence no variation in R_{K0} with t is observed. Closer to the transition, however, the time required to affect this conversion becomes long (critical slowing down) and hence the boundary layer in which this conversion takes place becomes thicker. Since the counterflow is incomplete in this boundary layer, part of the total heat current is diffusive, and hence a temperature gradient exists across this layer. Thus, R_{K0} is singular at T_λ, and close to T_λ measurements of R_{K0} show a dependence upon t. Many theorists have considered this effect.[20] Most recently Frank and Dohm[21] have calculated the singular part of R_{K0} from the dynamic renormalization-group theory.[22] Their prediction agrees well with our experimental data.[11] It contains no unknown parameters for the singularity. Only a constant additive and nonuniversal background resistance was adjusted in Ref. 21 in the comparison to our measurements.

Similar boundary layers due to slow dynamics exist in other superfluids, i.e., for ^{3}He and for superconductors.[23] Additionally, van Son *et al.* have proposed that a similar boundary effect may be observed at an interface between a half-metallic ferromagnet and a nonmagnetic electrical conductor.[24]

The second, and less well understood, phenomenon associated with the R_K anomaly at T_λ consists of a dependence of R_K on Q which is observed only for t less than a characteristic reduced temperature t_c. The value of t_c is well represented by a linear dependence on Q, and for $t < t_c$ the maximum slope $(\partial R_K/\partial Q)_t$ of $R_K(Q)$ is within the experimental resolution inversely proportional to t. For $t \ll t_c$ the value of $R_K(Q)$ saturates as Q is increased. The saturated value is approximately 0.4 cm^2 K/W above the value of the background resistance (which can be measured near $t \cong 10^{-2}$). To a good approximation, the saturation value is independent of Q. Data from other authors[15] on this nonlinear effect are in good agreement with our results. The physical origin of this effect is not

yet known.

In Sec. II below we discuss the apparatus and experimental procedures which we used to make measurements of $R_K(Q,t)$. Following this we present new and extensive data on $R_K(Q,t)$ in Sec. III.

II. EXPERIMENTAL ASPECTS

The main features of the cryostat used in these experiments have been described elsewhere.[25] Major modifications made to it included a new experimental cell design, together with a copper shield stage which completely surrounded the cell to protect it from black-body radiation from the thermally uncontrolled ^{4}He bath. Minor changes included a reduction in the intake flow impedance of the continuously operating ^{4}He refrigerator,[26] and the development of superconducting coaxial-cable heat sinks. The design and construction of the experimental liquid-helium cells, designated J, K, L_1, and L_2, are described in detail. The thermal conductivity of the copper stock used to make these cells is an important parameter in determining the Kapitza resistance. For this reason the thermal conductivity of the actual copper stock used to fabricate these cells was measured. The development and use of the much-higher-resolution thermometry crucial to this work would normally be included in this paper; however, this has become a major undertaking in its own right. All details concerning the development, use, and performance of these thermometers have been deferred to an upcoming publication. They are, however, already available in unpublished form.[13]

A. Overview of apparatus

1. Overview of cryostat

The cryostat used in this work is a modification of one described previously,[25] and is shown schematically in Fig. 1. The vacuum can, which was submerged in a liquid-helium bath at 4.2 K, contained four stages. Located on the first stage was a continuously operating ^{4}He refrigerator of the type described by De long *et al.*[26] It typically operated near 1.3 K and was used to cool the other stages in the cryostat.

As described in Ref. 26, the refrigerator operated by drawing liquid helium into its evaporation pot from the bath outside the cryostat through a flow impedance. This impedance was constructed by placing a 0.0246-cm-diameter stainless-steel wire into a stainless-steel capillary with an inner diameter of 0.0254 cm. Its length was 18 cm and its value measured with room-temperature helium was approximately 4×10^{11} cm^{-3}. A Nupro B-4F-0.5 flow filter[27] containing a piece of sintered metal made of 0.5-μm-diameter stainless-steel particles was used to filter the bath helium before it entered the impedance. All components of the Nupro filter were ultrasonically cleaned in acetone before assembly. Stycast 2850FT epoxy[28] was used to seal the sintered metal to the Nupro fitting.

The isothermal stage was suspended from the refrigerator stage by three hollow stainless-steel rods. When it was operated at 1.8 K, the heat current to the refrigerator stage was 4 mW. The temperature of this stage was then regulated to within a microKelvin of its operating temperature.

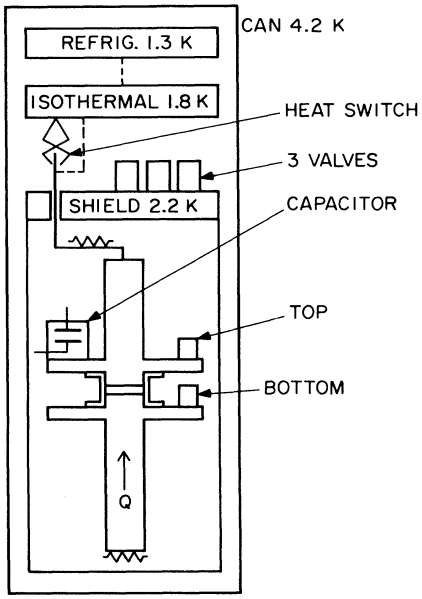

FIG. 1. Schematic diagram of the cryostat with cell K installed.

Below the isothermal stage was a copper shield stage which completely surrounded the experimental cell. This stage shielded the cell from radiation from the thermally uncontrolled bath at 4.2 K. Three hydraulically activated valves were located on this stage and were used to close off the cell fill capillary, as well as the supply capillaries to the two ^{3}He thermometers[25] during data acquisition in cells J and K. This stage was always operated above T_λ. A Cryo Cal CR-1000 germanium thermometer[29] and a 5-$k\Omega$ reference resistor were used in a five-wire bridge[30] to measure the shield-stage temperature. Like the isothermal stage, the shield was regulated to within a microKelvin of its set temperature.

Within the shield stage was the cell in which the actual measurements were made. It was thermally coupled to the warmer shield stage only through three hollow stainless-steel support rods which created a negligible heat input. The cell was connected to the isothermal platform by a 17.8-cm-long, 0.033-cm-diameter copper wire which provided a cooling power of about 30 μW. In addition, the cell could be cooled through a hydraulically activated heat switch which was thermally anchored to the isothermal stage and which when closed provided a cooling power to the cell of about 350 μW.

2. Experimental cells

Three different cells were used in this work. They are shown schematically in Figs. 2, 3, and 4. Cell J was constructed differently than cells K and L. Cells K and L,

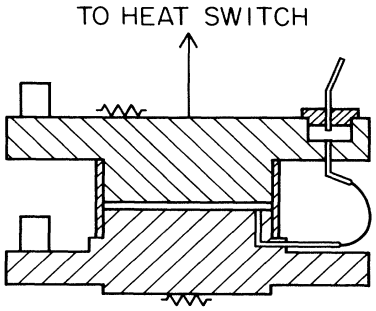

FIG. 2. Diagram of cell J shown in cross section.

which used the same solid endpieces, were made using a new construction technique described below. Cell L was cooled down twice and thus it is designated cell L_1 and cell L_2. Cells J, K, and L_1 used two thermometers with one on each copper endpiece of the cell. Cell L_2 had one additional thermometer located on a copper ledge which was compression fitted to the cell's stainless-steel sidewall half-way between the surfaces of the cell (see Fig. 3). Since no heat flowed through the interface between the midcell ledge and the helium, this midcell thermometer measured the true helium temperature T_{He} unaffected by helium-solid temperature jumps. This midcell thermometer of cell L_2 made it possible to measure the top and bottom Kapitza resistances individually while holding T_{He} constant. The physical dimensions of all the cells are listed in Table I.

The method of construction of cell J was quite similar to that of the cells described in Ref. 31. The cell endpieces were machined from oxygen-free, high-conductivity (OFHC) copper and the cell surfaces were lapped and polished to a mirror surface. The surfaces were then chemically plated with a layer of gold to protect them against oxidation.[32] The top endpiece contained a reservoir volume in which the helium liquid-vapor interface was maintained during the experiment (see Fig. 2). This insured that all measurements within cell J were made at saturated vapor pressure. A 0.005-cm inner-diameter capillary connected the reservoir volume to the fill line which was located in the bottom endpiece. The cell was assembled by slipping a 0.010-cm-thick stainless-steel ring around the copper endpieces. The ring was roughly 0.008 cm wider than the diameter of the endpieces. It was precisely machined to allow smooth, free slippage when rotated around the inserted endpieces. With the endpieces spaced with precision ground spacers, a ring of Stycast 1266 epoxy[28] was placed around the base of the wall ring. Surface tension drew the epoxy up between the stainless-steel wall ring and the copper endpiece sides until the epoxy reached the actual cell volume. After the epoxy dried the same procedure was repeated to epoxy the other endpiece to the wall ring and thus seal the cell. Since the low-viscosity epoxy flowed evenly between the copper endpieces and the stainless-steel sidewall, this assembly procedure guaranteed that all the volume between the sidewall and

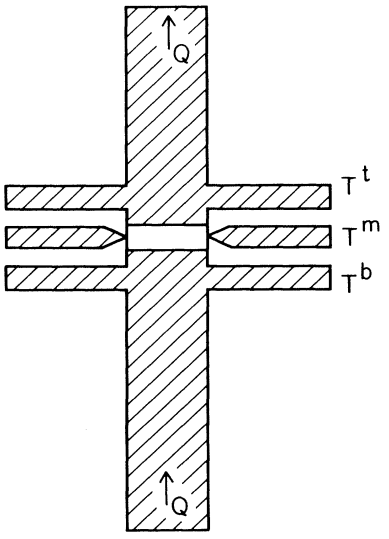

FIG. 3. Schematic diagram of cell L. Cell K used the same endplates as cell L but did not have a midplane ledge attached to the cell wall.

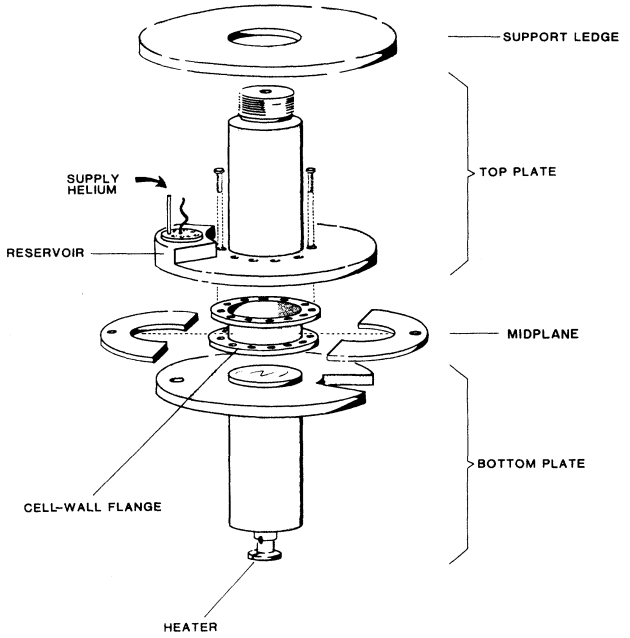

FIG. 4. Exploded view of cell L.

TABLE I. Room-temperature dimensions of the cells.

Cell	Diameter (cm)	Area (cm^2)	Height (cm)	D/H	Wall thickness (cm)
J	4.912±0.002	18.953±0.010	0.0975±0.0025	50.4	0.0107±0.0003
K	2.534±0.002	5.043±0.005	0.2878±0.0008	8.80	0.011±0.0018
L	2.534±0.002	5.043±0.005	0.576±0.0010	4.40	0.010±0.0013

the plates would be excluded from the helium during the experiment. The meniscus which the flowing epoxy formed at the cell volume was very small and did not reduce the cell's volume or the endplate's surface area by any significant amount.

A disadvantage of the cell J design was that the epoxy sealing the wall ring to the copper endpieces would weaken on repeated thermal cycling. Furthermore, the cell surfaces could not be preserved as the sidewall and epoxy were machined away. Hence the cell height could not be changed without repreparation of the cell surfaces. Thus a new method of cell assembly was developed and was used to construct cells K and L.

Cells K and L were prepared from the same endpieces, each of which was machined from a single piece of OFHC copper stock. This copper stock was very well characterized as will be explained below. The construction of cells K and L is shown schematically in Fig. 3. The cell endpieces consisted of 7.5-cm-long, 2.5-cm-diameter OFHC copper rods with thermometry ledges located approximately 0.3 cm from the end which formed the cell surface. The top endpiece contained a reservoir on its thermometry ledge. This reservoir had a volume of 0.183 cm^3 and contained a parallel-plate capacitor of diameter 1.09 cm with a spacing of 0.137 cm between its horizontally oriented plates. This resulted in a 0.6 pF nominal capacitance. During data acquisition the helium liquid-vapor interface was maintained between these capacitor plates, thereby insuring that the measurements were made at saturated vapor pressure. Using a General Radio model 1615A capacitance bridge, the interface was located to within 6 μm of its set position, corresponding to a capacitance resolution of roughly 10 aF. The fill capillary entered the reservoir, and the reservoir was connected to the active cell volume by a hole of 0.042-cm diameter. For a more detailed drawing of cells K and L see Fig. 4.

Each cell surface was lapped and polished to a mirror quality and then chemically plated with a 600-Å-thick layer of gold.[33] The side of the copper nub which elevated the cell surface from the thermometry ledge was then coated with a thin layer of pure indium using an ultrasonic soldering iron.[34] A stainless-steel wall flange was machined with an inner diameter within 2 μm of the outer diameter of the cell surfaces. Because of the close match between the diameters, the cell could not be assembled with the endpieces and wall flange at the same temperature. During assembly the endpiece was cooled to liquid-nitrogen temperature in a dry glovebox. At liquid-nitrogen temperature the diameter of the endpiece was 0.008 cm less than its room-temperature diameter. This allowed the room-temperature wall flange to be slipped on easily. The wall flange was screwed down evenly onto a 0.025-cm-diameter indium O ring located at the inner corner of the thermometry ledge. This same procedure was repeated to seal the other endpiece to the wall flange.

With the cell back at a uniform temperature the thin indium coating between the stainless-steel sidewall and the copper endpieces was under compression. This caused any empty volume to be filled by the flowing indium and hence to be inaccessible to the liquid helium during the experiment. The data taken in cell J agree well with the data from cells K and L. This indicates that this assembly technique was quite successful at excluding the volume between the sidewall and the copper from liquid helium.

3. *Thermal conductivity of copper*

Since the Kapitza resistances to be measured were small, the thermal resistance of the bulk copper between the gold cell surfaces and the thermometry stages could be as large as 25% of the total thermal resistance of the cell. For this reason we measured the thermal conductivity of the copper which was used to fabricate the endpieces of cells K and L. We removed two pieces of copper from the unneeded outer diameter of the stock which was used to make the endpieces. These copper pieces were then machined into two rods with diameters of 0.63 cm and lengths of 10.16 cm. One copper rod (rod A) was annealed by heating it to silver-soldering temperatures with a torch. After remaining at this temperature for about one minute it was allowed to return to room temperature slowly. The other rod (rod B) was only subjected to soft-soldering temperatures. The thermal conductivity of each rod was determined by passing a constant heat flux Q through it and measuring the resulting temperature difference ΔT between the top rod temperature T_H and the bottom rod temperature T_C. The temperature of the measurement was taken to be $(T_H+T_C)/2$. The thermal conductivity of each copper rod was obtained from

$$\lambda_{Cu}=QL/\Delta T\ .$$

Values of Q in the range $0.7<Q<11.6$ mW/cm^2 were used and no dependence of λ_{Cu} on Q was detectable. The results of the measurements of λ_{Cu} for rod B are shown in Fig. 5. The solid line is the best fit to the data with the result

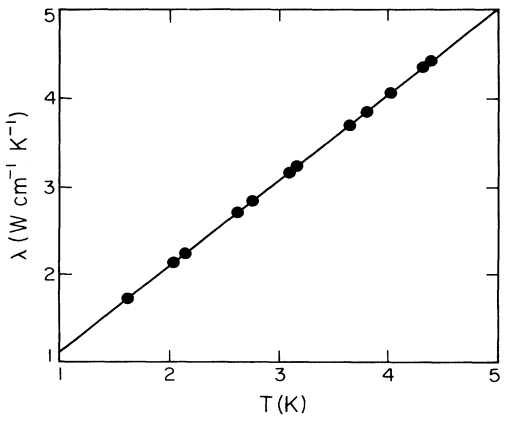

FIG. 5. Thermal conductivity of the oxygen-free, high-conductivity (OFHC) copper which was used to fabricate the endpieces used in cells K and L.

$$\lambda_{Cu}=(0.9734\pm0.0032)T+(0.1616\pm0.010)\ \text{W/cm K}$$

for rod B.

The thermal conductivity of rod A, which had been annealed as described above, also varied linearly with temperature. At 2 K the thermal conductivity of rod A was roughly a factor of 2 higher than that of rod B. The best fit to the rod A thermal conductivity resulted in

$$\lambda_{Cu}=(1.068\pm0.125)T+(1.463\pm0.038)\ \text{W/cm K}\ .$$

In this work, the endpieces of cells K and L were never heated above soft-soldering temperatures, so the thermal conductivities of rod B were used to correct the measurements described below. The rod A results serve as a warning that incidental heating of OFHC copper pieces during fabrication may increase their thermal conductivity by a significant amount.

B. Copper conductivity corrections

Cells K and L had a 6.35-cm length between the cell surfaces and the ends of the copper pieces at which the heat current was applied or removed. This insured that the isotherms within the copper would be flat in the regions between the thermometer location and the interface between the gold and the liquid helium.

In a numeric simulation designed to model the temperature profile within the cell L and cell K endplates, a 5.08-cm copper rod of 1.27-cell radius was placed against a 0.508-cm-thick layer of normal-fluid helium. An identical copper rod was located on the opposite end of the helium layer. Heat was applied to the center of the free end of one rod and removed at the center of the free end of the other. The copper thermal conductivity was 2.0 W/cm K. The helium conductivity was 1.8 mW/cm K, corresponding to HeI at saturated vapor pressure and 20 μK above T_λ. The effect of the boundary (Kapitza) resistances were included by adding a 0.127-cm-thick layer with a conductivity of 0.319 W/cm K. This corresponded to a boundary resistance of 0.4 cm^2 K/W, which was realistic for cells K and L. The simulation was set up with 0.127 cm between nodes in both the radial and longitudinal directions of the cylindrical coordinates. This method of solving the thermal diffusion equation discretely in cylindrical coordinates closely followed the method outlined by Ozisik.[35] The thermometry stages were not modeled in this simulation. They did not contain any heat sources or sinks and hence did not perturb the longitudinal heat flow away from their location.

In the simulation, 50.67 μW of heat entered one copper rod and a corresponding 50.67 μW was removed from the copper rod on the opposite side of the helium layer. This corresponded to an average heat current of 10 μW/cm^2 through the copper which would create a 25.4-μK temperature difference along the 5.08-cm copper rod if the heat flow were uniform across the rod's diameter. The heat-flow model was iterated until a radial temperature variation of less than 10^{-8} K could be detected. At a distance of 1.27 cm along the length of the rod from the heated end, the total temperature variation across the radius of the rod was 300 nK, which was 1.2% of the total temperature difference along the 5.08-cm length of the rod. At 2.04 cm from the heated end the radial temperature variation was down to 9 nK, which was 0.035% of the temperature difference along the length. Hence to insure flat isotherms at the cell surface to the minimum level resolvable using this simulation one should use an OFHC copper rod with an aspect ratio (diameter/length) of 1 or less to separate the heater from the liquid-helium layer. Since in cells K and L the copper aspect ratio was 0.4, these copper isotherms were very flat at the liquid-helium interface and hence effects associated with radial thermal gradients in the copper would not be seen in cells K and L.

The thermal conductivity of rod B was used to evaluate the contribution from the copper ends (typically 25%) to the measured temperature differences ΔT for cells K and L during Kapitza-resistance measurements described below. This contribution is given by $\Delta T_{Cu}=L_{Cu}Q/\lambda_{Cu}$, where $L_{Cu}=1.044$ cm is the total length of the copper sections between the thermometers, and Q is the heat current through the cell. For cell J a correction was estimated by subtracting a contribution ΔT_{Cu}, which yielded overall agreement with the cell-K data. The required ΔT_{Cu} differed by only 24% from a rough *a priori* estimate based on the geometry of cell J and the λ_{Cu} of the copper stock used in cell K.

C. Experimental procedure

The singularity in the zero-power limit of R_K was not resolved in previous work using conventional germanium thermometry.[9,31] Its quantitative study required the extremely high-resolution thermometers which have been developed only recently.[13,25,36,37] Our measurements were made using several cells and two different methods of thermometry. Cell-J and cell-K measurements were

made with thermometers which detected the variation of liquid ^{3}He vapor pressure with temperature[25] using a very sensitive capacitive strain gauge technique.[38,39] The thermometers used with cell L detected the change in the paramagnetic susceptibility with temperature of copper ammonium bromide (CAB), a salt with a Curie temperature 0.4 K below T_λ at saturated vapor pressure (SVP).[40] Both techniques of thermometry were virtually free from Johnson noise and could be driven at much higher bridge voltages than the germanium thermometers without substantial heating. Both the ^{3}He vapor-pressure thermometers and the CAB thermometers were capable of resolving a few nK in temperature changes near T_λ, and thus had roughly 2 orders of magnitude more resolution than the best commercially available thermometers near 2 K. The bulk superfluid transition of the pure ^{4}He in the cell served as a fixed point.

The Kapitza resistance was measured by applying a heat flux Q to the bottom of the cell while maintaining the top thermometer at a constant temperature T^t. The resulting rise of the bottom-plate temperature $\Delta T(Q)$ was used[41] to evaluate the Kapitza resistance

$$R_K=(\Delta T-\Delta T_{\mathrm{Cu}})/2Q \tag{1}$$

in cells J, K, and L_1. The temperature assigned to this measurement was $T^t+\Delta T/2$. In cell L_2 we measured and regulated the actual helium temperature T^{He} with the midcell thermometer (see Fig. 3). This allowed us to measure the Kapitza resistance of the top and bottom surfaces independently. Hence in cell L_2

$$R_K^i=(\Delta T^i-\Delta T^i_{\mathrm{Cu}})/Q\ , \tag{2}$$

where i designates the top or bottom endplate, ΔT^i is the change of the top or bottom temperature when the heat flux Q is applied, and ΔT^i_{Cu} is the copper contribution to the observed temperature differences at the respective endplate. For the temperature corresponding to these measurements we chose the mean temperature $\bar{T}=T_t+\Delta T/2$ in cells J, K, and L_1, and the actual helium temperature T_{He} which was directly measured with the midcell thermometer in cell L_2. Since the superfluid transition temperature at a given level in the liquid was suppressed by the hydrostatic pressure due to the liquid above, there existed a variation of T_λ along the vertical axis of the cell.[42] We used T_λ at the middle of the liquid layer to define the reduced temperature $t\equiv 1-\bar{T}/T_\lambda$ for all the cells.

Measurements made in cells J, K, and L_1 were taken manually, cell-L_2 measurements were fully automated using a computer located outside the shielded room. Ultrapure ^{4}He with a measured ^{3}He impurity concentration of 5×10^{-10} was used in cells K and L.[43] Standard well helium was used in cell J.

The Kapitza resistance has been observed to vary greatly between nominally identical surfaces in different measurements.[3,9] In fact Dingus *et al.*[9] report that the polished copper surfaces in their cell have a Kapitza resistance which varies by up to 30% on thermal cycling to only 77 K. Hence we do not expect our measurements of R_K to repeat from one cell to the next, even though the surface preparations are similar. In the data discussed below we allow for this variation by adding small offsets to the data from cells J and L to make them coincide with the cell K data at $t=2\times10^{-3}$, where the singular and nonlinear effects are smaller than our thermometry resolution can detect. Unlike the total size of R_K, we show below that the singularity in R_K and the nonlinear dependence of R_K on Q gave quite repeatable results from run to run. Comparison with the work of others[44] suggests that the Q dependence of R_K is insensitive to the solid surface material and its preparation. The sizes of the $Q=0$ singularity of R_K reported by other authors vary considerably from our result, suggesting the need for further measurements.

Prior to making measurements of R_K within cell K, measurements of the thermal conductivity within the normal-fluid phase were made. These normal-fluid measurements agreed very well with those of Tam and Ahlers,[31] indicating that the cell-K geometry was well known and that there were no major systematic discrepancies between the sets of measurements.

III. RESULTS

Shown in Fig. 6 are cell-K measurements of R_K plus 0.033 cm^2 K/W plotted against Q at nine values of $\log_{10}t$, and cell L_1 measurements plus 0.023 cm^2 K/W at $\log_{10}(t)=-4.13$. Notice that as t becomes small, the Q dependence of the data at constant t becomes very strong, and that the zero-Q limit of R_K, designated R_{K0}, increases with decreasing t.

The dependence of R_{K0} on $\log_{10}(t)$ in cell K and cell J is displayed in Fig. 7. For $t<4\times10^{-6}$ the Q dependence was so strong that extrapolation to $Q=0$ was not attempted. For $t>4\times10^{-6}$, the Q-independent region was accessible with our thermometer resolution, and measurements in the $Q=0$ limit were made. The steep increase of R_{K0} at the large values of t is similar to that which has been observed by many other authors.[3,4,6,31,44] It corre-

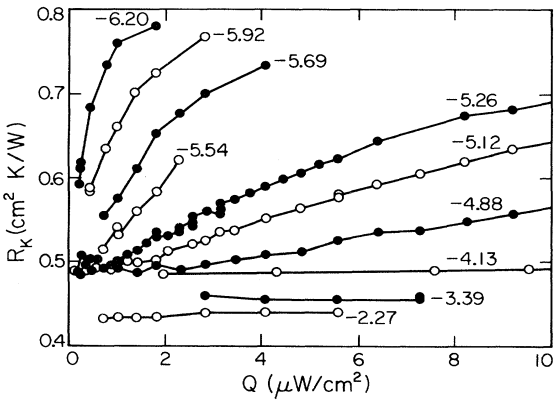

FIG. 6. Kapitza resistance measurements vs heat-flux Q at constant reduced-temperature $t\equiv1-T/T_\lambda$. Values of $\log_{10}(t)$ are shown in the insets. All points are cell-K data plus 0.033 cm^2 K/W except for the data at $\log_{10}t=-4.13$, which are cell L_1 data plus 0.023 cm^2 K/W.

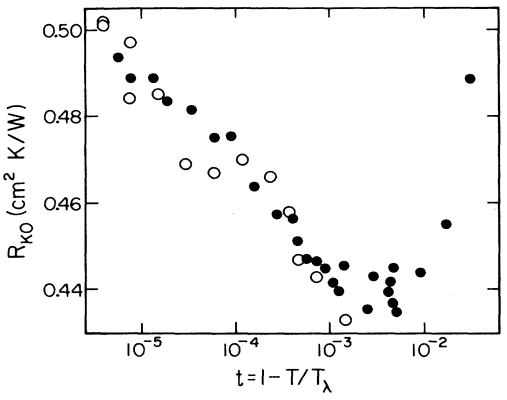

FIG. 7. Kapitza resistance measurements R_K in the limit $Q\rightarrow 0$ vs t. Solid circles are cell-K measurements plus 0.033 cm^2 K/W, open circles are uncorrected cell-J measurements minus 0.587 cm^2 K/W.

sponds to the regular dependence of R_{K0} upon T, which can be written approximately as $R_{K0}\propto T^{-3}$. Unfortunately, very few measurements of R_{K0} were taken in cell K at values of $t > 10^{-2}$.

If R_{K0} were a regular function of temperature through T_λ, then the R_{K0} measurements displayed in Fig. 7 would approach a constant value near 0.44 cm^2 K/W as t vanishes, say for $t \lesssim 10^{-3}$. We see that this is not the case: measurements of R_{K0} increase by 10% as t decreases from 10^{-3} to 10^{-5}, indicating that R_{K0} is singular at T_λ. Notice in Fig. 7 that the cell-K and cell-J results show the same singularity in R_K. Since the spacing of cells K and J differed greatly (see Table I), we conclude that the singularity displayed in Fig. 7 is due to an effect near the solid surfaces and is independent of the bulk helium. Furthermore, similar singularities were observed in cell L on both thermal cyclings. The same singularity was observed within cells J and K, which had different endplates. This suggests that the observed effects are independent of the surface detail and preparation.

Recently, Frank and Dohm[21] calculated the singularity in R_{K0} using a renormalization-group method[22] and model F of Halperin *et al.*[45] for the dynamics of the superfluid transition. In their theory, all adjustable parameters had been determined previously by a fit of their predictions for the thermal conductivity of ^{4}He above T_λ (Ref. 46) to experimental data.[31] The only remaining parameter required for a comparison with experiment is the additive background value, which apparently differs for different surfaces. In Fig. 8(a) we compare our data for R_{K0} with the calculation. The theoretical curve was shifted vertically so as to cause agreement in the range $10^{-3}\lesssim t\lesssim 10^{-2}$ where the singular contribution to R_{K0} is nearly negligible. Although the theoretical curve falls slightly below the data for $\log_{10}t \lesssim -3.5$, the agreement is clearly quite good over the entire experimentally accessible range of t. The small systematic differences are well within possible systematic errors in the theory or the experiment.

Measurements of R_K for small t made by other groups[7,9,12,15,17] have also shown the existence of an anomaly in R_K at T_λ. The data of Zhong *et al.*[17] display a singularity in R_{K0}, but with an amplitude several times larger than that which we report here. This is shown in Fig. 8(b), where their results are plotted with the same vertical resolution as our data in Fig. 8(a). The line represents the calculation by Frank and Dohm, again displaced vertically so as to cause agreement for $10^{-3}\lesssim t\lesssim 10^{-2}$. Clearly, the data of Zhong *et al.* do not agree well with the theory. They rise much more rapidly than ours as t vanishes. Although the authors do not claim that their data correspond to the $Q=0$ limit, their results also increase more rapidly with decreasing t than do ours at similar power densities (see Fig. 9 below). We note that the active area across which the current left the helium was not as precisely defined in the cell used by Zhong *et al.* This is because there was a capacitor situat-

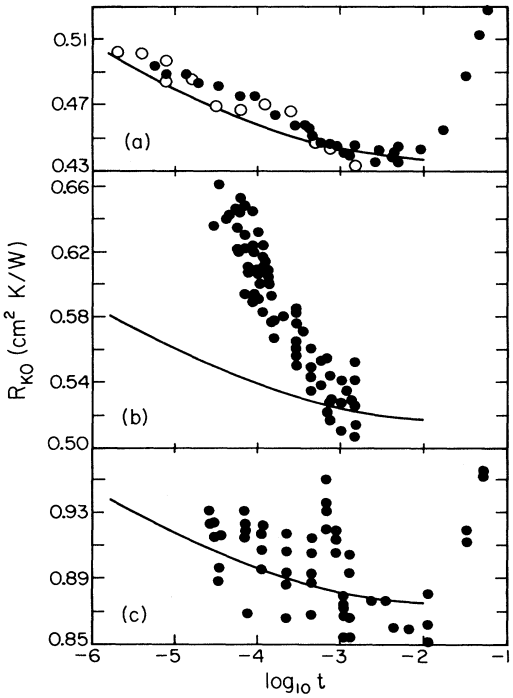

FIG. 8. Comparison of experimental measurements at relatively low power densities where the power dependence is at most weak, with the theoretical result of Frank and Dohm (Ref. 21) for the singular part of R_{K0}. In each case, the theoretical curve (solid line) is moved vertically so as to agree with the background resistance of the experiment in the range $10^{-3}\lesssim t\lesssim 10^{-2}$. (a) The zero-power limit R_{K0} of R_K reported in this paper. (b) Data from Figs. 7 and 8 of Zhong *et al.* (Ref. 17) (the authors do not assert that these data correspond to the zero-power limit). (c) Results of Tam and Ahlers (the authors do not assert that these data correspond to the zero-power limit) (Ref. 31).

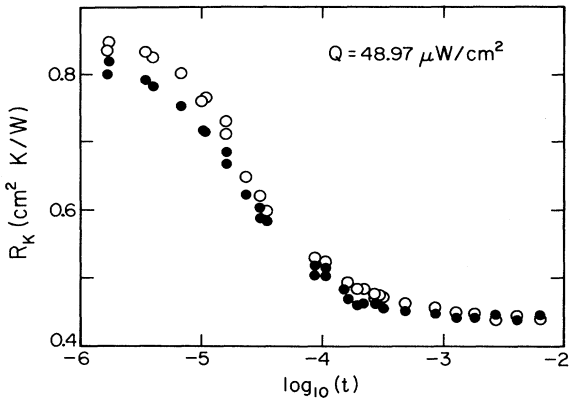

FIG. 9. Simultaneous measurements from cell L_2 of the Kapitza resistance R_K of the top plate (solid points) and the bottom plate (open points) plotted against $t \equiv 1 - T_{\rm He}/T_\lambda$.

ed above the top plate of their cell, which sampled the fluid by means of an array of small holes through this plate. Some heat might have flown into the top main body of the cell via these small holes. Also, their cell consisted of cylindrical pieces with parallel faces which snugly fitted into the stainless-steel wall. A large sidewall area did therefore exist through which some of the heat might have been flowing. However, Zhong *et al.*, on the basis of several experiments, argued that only the plate area perpendicular to the heat flux on the cell was the active area, since the ratio $\Delta T/Q$ did not change substantially with Q, nor with the concentration of ^{3}He impurities. In our cell, sidewall areas were eliminated. A singularity in R_{K0} as large as that reported by Zhong *et al.* should also have been detected by Tam and Ahlers.[31] Their results, together with the theoretical calculation (displaced vertically so as to cause agreement for $10^{-3} \lesssim t \lesssim 10^{-2}$) are shown in Fig. 8(c). The authors rightly concluded that their data provide no definitive evidence for a singularity in R_{K0}. However, as can be seen in Fig. 8(c), there is a slight upward trend in the data as t becomes small, and the size of this trend is quite consistent with the size of the calculated effect. The data of Tam and Ahlers are inconsistent with a singularity in R_{K0} as pronounced as that indicated by the data of Zhong *et al.* [Fig. 8(b)].

Our thermometry resolution allowed us to make measurements with an accuracy of 2% or better at currents as small as 0.45 μW/cm^2, corresponding to a temperature jump due to R_K of about 200 nK. Hence our zero-Q limit corresponds to values of Q on the order of this minimum heat flux. Recently Li *et al.*[47] have made measurements of R_K over the range $10^{-6} \le t \le 10^{-3}$ with a much smaller heat flux $Q = 0.05$ μW/cm^2. Their results using this value of Q show no singularity in R_{K0} over this range in t. Thus, their results differ from ours and from those of Zhong *et al.*[15] and Chui *et al.*[12] They also differ from the theoretical result of Frank and Dohm.[21] Hopefully Li *et al.*[47] will repeat their measurements in this range of t at numerous values of Q between 0.05 and 10 μW/cm^2. This may resolve the discrepancy between the data sets.

In cell L_2 we could measure and regulate the actual helium temperature $T_{\rm He}$ with our midcell thermometer. Hence we could measure the Kapitza resistance of the top and bottom plates independently. Figure 9 shows a comparison of the top-plate (solid points) and the bottom-plate (open points) Kapitza resistances[48] for $Q = 48.97$ μW/cm^2. In Fig. 9 the reduced temperature t is simply defined as $1 - T_{\rm He}/T_\lambda$, as mentioned above. Notice that the data at small t show an apparent departure of the top- and bottom-plate measurements from each other, with the bottom-plate measurements falling systematically higher. Since all previous experimental evidence suggests that this dependence of R_K on Q is associated with thin liquid-helium layers near the solid surfaces, we defined an effective reduced temperature t^* as

$$t^* = 1 - (T_{\rm He} + \Delta T_b^s/2)/T_{\lambda,b} \quad \text{(bottom surface)}, \tag{3a}$$

$$t^* = 1 - (T_{\rm He} - \Delta T_t^s/2)/T_{\lambda,t} \quad \text{(top surface)}, \tag{3b}$$

for the top and bottom boundary layers. In Eqs. (3a) and (3b) the boundary-layer temperature-variations ΔT_b^s and ΔT_t^s are determined by multiplying the heat-flux Q by the amount of the Kapitza resistance which is above the background Kapitza resistance at $t = 2 \times 10^{-3}$. Figure 10 displays the same data shown in Fig. 9 but plotted against t^*. Although the variation of R_K with t^* is the same within our resolution for the top and bottom plates, the magnitude of $R_{K,b}$ was larger than $R_{K,t}$. This may be due to the cell fill hole which enters through the top plate. Notice that the top- and bottom-plate measurements agree well when plotted against t^*. Five sets of constant heat-current measurements (including the set displayed in Figs. 9 and 10) were made spanning the range $9.79 \le Q \le 48.97$ μW/cm^2 in even intervals. All these data sets show the same Q dependence at the top and bottom plates only when the data are plotted against t^*.

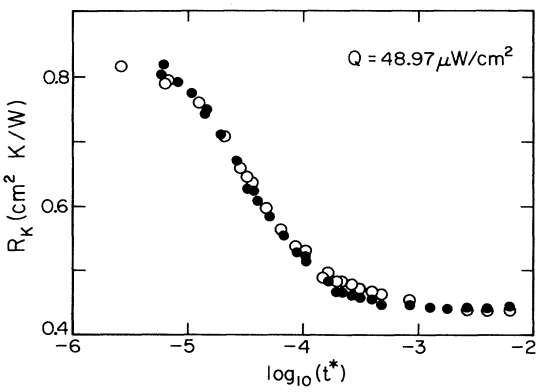

FIG. 10. Data displayed in Fig. 9 replotted vs t^*. Notice that the apparent discrepancy between the top and bottom R_K measurements for small t displayed in Fig. 9 are accounted for nicely by this redefinition [t^*, see Eqs. (3a) and (3b)] of the reduced temperature.

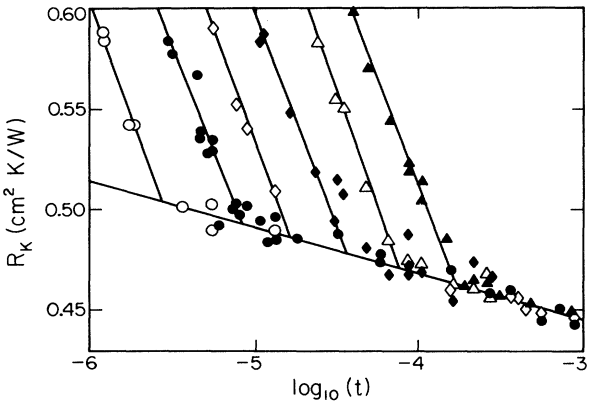

FIG. 11. Measurements of the Kapitza resistance R_K vs $\log_{10}t$ at six values of Q: open circles, 0.45; solid circles, 1.81; open diamonds, 4.08; solid diamonds, 9.79; open triangles, 19.59; solid triangles, 39.18 μW/cm^2. For $Q \leq 4.08$ μW/cm^2 the data are from cell K. The data for $Q \geq 9.79$ μW/cm^2 are measurements from the top surface of cell L_2 minus 0.016 cm^2 K/W. The reduced temperature at which the line through the Q-independent data intersects with the line through the constant-Q data is designated t_c for that value of Q.

Figure 11 shows additional measurements of R_K versus $\log_{10}(t)$ at six values of Q. The data displayed in Fig. 11 are from cell K for $Q \leq 4.08$ μW/cm^2. The points in Fig. 11 with $Q \geq 9.79$ μW/cm^2 are measurements from the top surface of cell L_2 minus 0.016 cm^2 K/W. Since we have no theoretical guidance about the functional form of $R_K(Q)$, we now proceed with a phenomenological description of the experimental data. Notice that the reduced temperature at which the data begin to show a dependence on Q is itself dependent on Q. Thus, we define a characteristic reduced-temperature $t_c(Q)$ as illustrated in Fig. 11. We simply draw a line through the Q-independent points and intersect this line with another drawn through constant-Q points within the Q-dependent region where $R_K(Q)$ versus $\log_{10}(t)$ has approximately attained a constant slope. The reduced temperature at which these two lines intersect was designated t_c for that value of Q. This procedure neglects any gradual growth of the Q-dependent contribution to R_K with decreasing t which may be associated with a gradual onset for this effect. Figure 12 displays t_c versus Q on logarithmic scales. Our data from cell K are shown as solid triangles, while our data from the top endplate of cell L_2 are displayed as solid circles. The open triangles are data inferred from Fig. 4(b) of Dingus *et al.*[9] and the open squares are inferred from the data within Fig. 4 of Chui *et al.*[12] Both Chui *et al.*[12] and Dingus *et al.*[9] used copper surfaces within their cells. Most recently, Zhong *et al.*[15] report agreement with these results for their first series of measurements, but their second data series falls below the line indicated in Fig. 12. The agreement of t_c from their cells with our measurements which were made using gold surfaces strongly suggests that this effect is independent of the exact surface material and its preparation. This, together with the observation that the Q dependence is independent of the cell spacing, suggests strongly that these effects are associated with a thin hydrodynamic layer in the helium near the solid boundaries. The line shown in Fig. 12 is the best fit of the solid points to

$$\log_{10}(t_c)=\alpha+\beta\log_{10}(Q)\ . \tag{4a}$$

This fit gave $\alpha=-5.275\pm0.046$ and $\beta=0.914\pm0.038$ for Q in units of μW/cm^2. Here the error estimates are the 67% confidence limits. Since $\beta\cong1$, t_c is approximately proportional to Q. Assuming $\beta=1$, we obtain

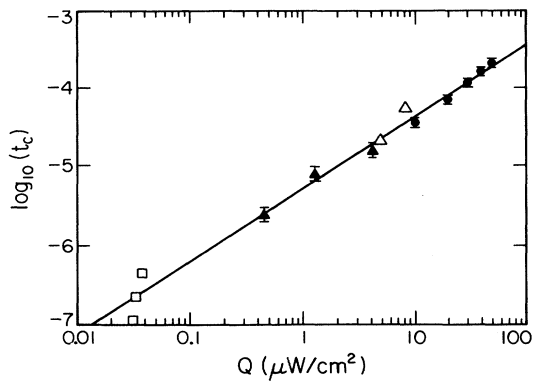

FIG. 12. $\mathrm{Log}_{10}(t_c)$ vs Q. The solid points are our measurements from cell K (triangles) and from the top plate of cell L_2 (circles). The open squares are inferred from Fig. 4 of Chui *et al.* (Ref. 12) and the open triangles are inferred from Fig. 4(b) of Dingus *et al.* (Ref. 9). The line is the best fit of $\log_{10}(t_c)=\alpha+\beta\log_{10}(Q)$ to the data. Since $\beta\approx1$, $t_c\sim Q$.

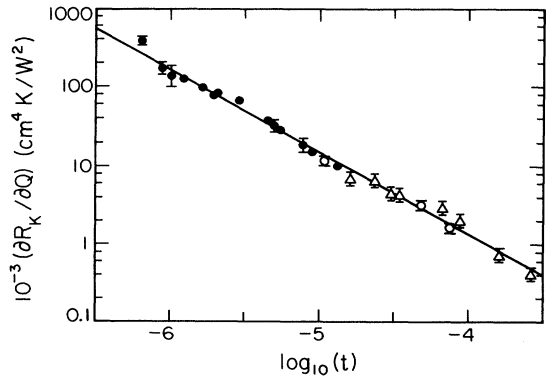

FIG. 13. The maximum slope $S\equiv(\partial R_K/\partial Q)_t$ of the Kapitza resistance measurements vs t for $t<t_c(Q)$. The solid points are measurements from cell K, while the open circles are from cell L_1 and the open triangles are from the top plate of cell L_2. The line is the best fit of $\log_{10}S=a+b\log_{10}(t)$ to the data. Since $b\approx-1$, $S\sim1/t$.

$$t_c = Q/Q_0 \ , \tag{4b}$$

with $Q_0 = 0.288$ W/cm^2 from the data represented by the solid points in Fig. 12.

We see from Fig. 6 that for $t < t_c(Q)$ measurements of R_K show a maximum slope $S = (\partial R_K/\partial Q)_t$ which becomes larger as t becomes smaller. Figure 13 displays the maximum value of S versus t. The solid points in Fig. 13 are from cell K, while the open circles are from cell L_1, and the open triangles are from the top surfaces of cell L_2. The solid line in Fig. 13 is the best fit of

$$\log_{10}(S) = a + b \log_{10}(t) \tag{5a}$$

to the data from all the cells. The result of this fit gave $a = -1.034 \pm 0.095$ and $b = -1.041 \pm 0.0184$ with S in units of cm^4 K/W^2. Here again the error estimates are 67% confidence limits. Since $b \cong -1$, S is approximately proportional to $1/t$. Assuming $b = -1$, we obtain

$$S = k/t \ , \tag{5b}$$

with $k = 0.12$ cm^4 K/W^2.

The results of Eqs. (4b) and (5b) suggest that there is a range of t below but near $t_c(Q)$ over which the nonlinear contribution

$$R_{KQ} = R_K - R_{K0} \tag{6}$$

to R_K can be written as a function of the single variable q/t, with $q = Q/Q_0$. We find that this is indeed the case over the *entire* range of q/t. This is illustrated in Fig. 14, where R_{KQ} is plotted as a function of $\ln(q/t)$ for several values of Q. As already apparent from Fig. 6, the data in Fig. 14 suggest that R_{KQ} saturates at a constant, Q-independent value as q/t becomes large. The saturation value is approximately equal to 0.35 cm^2 K/W, and is consistent with the measurements of Zhong *et al.*[15–17]

In conclusion, a singular contribution to the Kapitza resistance has been observed which is independent of the heat-flux Q which was used to make the measurement. A theoretical prediction[21] for this singular boundary resistance based on the dynamic renormalization-group theory and containing no adjustable parameters agrees well with our data. In addition, a strong nonlinear dependence of the Kapitza resistance on Q has been observed. Comparison of our results to the results of other authors shows good repeatability. Unfortunately, the physical origin of this Q-dependent effect is not yet understood. We find that the Q-dependent contribution to R_K can be represented by a function of the single variable Q/t.

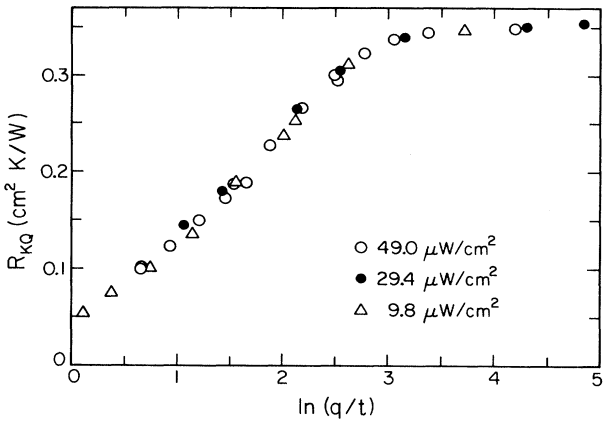

FIG. 14. The Q-dependent contribution R_{KQ} to R_K as measured in cell L_2 as a function of $\ln(q/t)$, where $q = Q/Q_0$ with $Q_0 = 0.288$ W/cm^2.

ACKNOWLEDGMENTS

We are grateful to V. Dohm, R. Ferrell, and H. Meyer for helpful discussions. This work was supported by the National Science Foundation under Grants No. DMR84-14804 and DMR89-18393.

*Present address: Electrical Standards Division 7342, Sandia National Laboratories, Albuquerque, NM 87185.

[1]I. M. Khalatnikov, *An Introduction to the Theory of Superfluidity* (Benjamin, New York, 1965).

[2]P. L. Kapitza, J. Phys. (Moscow) **4**, 181 (1941). A brief mention of a boundary resistance had been made earlier by W. H. Keesom and A. P. Keesom, Physica (Utrecht) **3**, 359 (1936).

[3]Gerald L. Pollack, Rev. Mod. Phys. **41**, 48 (1969).

[4]J. Pfotenhauer and R. J. Donnelly, Adv. Heat Transfer **17**, 65 (1985).

[5]E. T. Swartz and R. O. Pohl, Rev. Mod. Phys. **61**, 605 (1989).

[6]Eric Thomas Swartz, Ph.D. thesis, Cornell University, Ithaca, New York (1987).

[7]D. White, O. D. Gonzales, and H. L. Johnston, Phys. Rev. **89**, 593 (1953).

[8]R. Duncan, G. Ahlers, and V. Steinberg, Bull. Am. Phys. Soc. **31**, 281 (1986).

[9]M. Dingus, F. Zhong, and H. Meyer, J. Low Temp. Phys. **65**, 185 (1986).

[10]R. Duncan and G. Ahlers, Jpn. J. Appl. Phys. Suppl. **26-3**, 363 (1987).

[11]R. V. Duncan, G. Ahlers, and V. Steinberg, Phys. Rev. Lett. **58**, 377 (1987).

[12]T. C. P. Chui, Q. Li, and J. A. Lipa, Jpn. J. Appl. Phys. Suppl. **26-3**, 371 (1987).

[13]Robert V. Duncan, Ph.D. thesis, University of California, Santa Barbara, CA (1988).

[14]Q. Li, T. C. P. Chui, and J. A. Lipa, Bull. Am. Phys. Soc. **33**, 1373 (1988).

[15]F. Zhong, J. Tuttle, and H. Meyer, in *Proceedings of Conference on Quantum Fluids and Solids—1989,* AIP Conf. Proc. No. 194, edited by Gary G. Ihas and Uasumasa Takano (AIP, New York, 1989).

[16]F. Zhong, Ph.D. thesis, Duke University, Durham, North Carolina (1989).

[17]F. Zhong, J. Tuttle, and H. Meyer, J. Low Temp Phys. **79**, 9 (1990).

[18]Other measurements (Refs. 12, 15–17) of R_{K0} show consider-

ably different values for the strength of this singularity, and as of now this discrepancy between different experiments has not been resolved.

[19]L. D. Landau, J. Phys. (Moscow) **5**, 71 (1941), Sec. 6.

[20]C. J. Gorter, in *Proceedings of the Second International Conference on Low Temperature Physics* (Oxford University Press, Oxford, England, 1951), p. 97; R. de L. Kronig, *ibid.*, p. 99; C. J. Gorter, K. W. Takonis, and J. J. M. Beenakker, Physica (Utrecht) **17**, 841 (1951); R. A. Ferrell (unpublished); W. M. Saslow, Phys. Lett. **35A**, 241 (1971); V. L. Ginzburg and A. A. Sobyanin, Usp. Fiz. Nauk. **120**, 153 (1976); [Sov. Phys. Usp. **19**, 773 (1976)]; D. Frank, M. Grabinski, V. Dohm, and M. Liu, Phys. Rev. Lett. **60**, 2336 (1988); S. J. Putterman, *Superfluid Hydrodynamics* (North-Holland, Amsterdam, 1974); A. Onuki, Progr. Theor. Phys. Suppl. **79**, 191 (1984); P. H. Roberts and R. J. Donnelly, Annu. Rev. Fluid Mech. **6**, 179 (1974); M. Grabinski and M. Liu, Phys. Rev. B **40**, 8720 (1989).

[21]D. Frank and V. Dohm, Phys. Rev. Lett. **62**, 1864 (1989).

[22]K. G. Wilson, Phys. Rev. B **4**, 3174 (1971); **4**, 3184 (1971). For a review, see J. Kogut and K. G. Wilson, Phys. Rep. **12C**, 76 (1974); or M. E. Fisher, Rev. Mod. Phys. **46**, 597 (1974). For a review of the applications to transport properties, see P. C. Hohenberg and B. I. Halperin, Rev. Mod. Phys. **49**, 435 (1977).

[23]J. P. Eisenstein and R. E. Packard, Phys. Rev. Lett. **49**, 564 (1982); and subsequently interpreted by H. Brand and M. C. Cross, Phys. Rev. Lett. **49**, 1959 (1982). For superconductors, a related effect has been proposed by T. J. Rieger, D. J. Scalapino, and J. E. Mercereau, Phys. Rev. Lett. **27**, 1787 (1971); and observed by M. L. Yu and J. E. Mercereau, Phys. Rev. Lett. **28**, 1117 (1972). See also J. Clarke, Phys. Rev. Lett. **28**, 1363 (1972); and a review of similar effects by J. Clarke, see J. Clarke, in *Modern Problems in Condensed Matter,* edited by D. N. Landenberg and A. I. Larkin (North-Holland, New York, 1986), Vol. 12, p. 1–64.

[24]P. C. van Son, H. von Kampen, and P. Wyder, Phys. Rev. Lett. **58**, 2271 (1987).

[25]V. Steinberg and G. Ahlers, J. Low Temp. Phys. **53**, 255 (1983).

[26]L. E. de Long, O. G. Symko, and J. C. Wheatley, Rev. Sci. Instrum. **42**, 147 (1971).

[27]Nupro Company, 4800 E. 345th Street, Willoughby, OH 44094.

[28]Emerson and Cumming, Inc., Northbrook, IL; Canton, MA; and Gardena, CA.

[29]Cryo Ccal, Inc., 2457 University Avenue, St. Paul, MI 55114.

[30]K. H. Mueller, G. Ahlers, and F. Pobell, Phys. Rev. B **14**, 2096 (1976).

[31]W. Y. Tam and G. Ahlers, Phys. Rev. B **32**, 5932 (1985).

[32]Atomex Immersion Gold, Engelhard Industries Division, Engelhard Minerals and Chemicals Corp., 2655 U.S. Route 2, Union, NJ 07083.

[33]This 600 Å thickness is the maximum deposit according to Fig. 7 of Engelhard's product documentation for Atomex Immersion Gold. See Ref. 32.

[34]FibraSonics, Inc., 5312 N. Elston, Chicago IL 60630, Model G-35 ultrasonic soldering iron.

[35]M. Necati Ozisik, *Boundary Value Problems of Heat Conduction* (International Textbook, Scranton, PA, 1968).

[36]J. Lipa, B. C. Leslie, and T. C. Walstrom, Physica (Amsterdam) **107B**, 331 (1981); T. C. P. Chui and J. A. Lipa, in *Proceedings of the Seventeenth International Conference on Low Temperature Physics,* edited by U. Eckern, A. Schmid, W. Weber, and H. Wühl (North-Holland, Amsterdam, 1984), p. 931.

[37]R. V. Duncan and G. Ahlers (unpublished).

[38]G. C. Straty and E. D. Adams, Rev. Sci. Instrum. **40**, 1393 (1969).

[39]D. S. Greywall and P. A. Busch, Rev. Sci. Instrum. **51**, 509 (1980).

[40]L. J. de Jongh, A. R. Miedema, and R. F. Wielinga, Physica **46**, 44 (1970).

[41]The temperature difference ΔT_{II} across the bulk superfluid due to dissipative processes was calculated and found to be negligible ($\Delta T_{II}/\Delta T \lesssim 10^{-6}$; see also Ref. 9).

[42]G. Ahlers, Phys. Rev. **171**, 275 (1968).

[43]United States Department of the Interior, Bureau of Mines, Helium Operations, 1100 S. Fillmore, Amarillo, TX 79101.

[44]D. White, O. D. Gonzales, and H. L. Johnston, Phys. Rev. **89**, 593 (1953); M. Dingus, F. Zhong, and H. Meyer, J. Low Temp. Phys. **65**, 185 (1986); T. C. P. Chui, Q. Li, and J. A. Lipa, Jpn. J. Appl. Phys. Suppl. **26-3**, 371 (1987).

[45]B. I. Halperin, P. C. Hohenberg, and E. D. Siggia, Phys. Rev. B **13**, 1299 (1976).

[46]V. Dohm, Z. Phys. B **60**, 61 (1985); **61**, 193 (1985).

[47]See Q. Li, T. C. P. Chui, and J. A. Lipa, Bull. Am. Phys. Soc. **33**, 1373 (1988) for a report on experimental results which differ from that of Ref. 12.

[48]For the comparison shown in Figs. 9 and 10, 0.28 and 0.02 cm^2 K/W was subtracted from R_K for the top and bottom surfaces, respectively, to achieve agreement at large t with the cell-K data shown in Fig. 7.